



HAL
open science

Rigid Point-Surface Registration using Oriented Points and an EM Variant of ICP for Computer Guided Oral Implantology

Sébastien Granger, Xavier Pennec, Alexis Roche

► **To cite this version:**

Sébastien Granger, Xavier Pennec, Alexis Roche. Rigid Point-Surface Registration using Oriented Points and an EM Variant of ICP for Computer Guided Oral Implantology. RR-4169, INRIA. 2001. inria-00072453

HAL Id: inria-00072453

<https://inria.hal.science/inria-00072453>

Submitted on 24 May 2006

HAL is a multi-disciplinary open access archive for the deposit and dissemination of scientific research documents, whether they are published or not. The documents may come from teaching and research institutions in France or abroad, or from public or private research centers.

L'archive ouverte pluridisciplinaire **HAL**, est destinée au dépôt et à la diffusion de documents scientifiques de niveau recherche, publiés ou non, émanant des établissements d'enseignement et de recherche français ou étrangers, des laboratoires publics ou privés.

***Rigid Point-Surface Registration using Oriented
Points and an EM Variant of ICP for Computer
Guided Oral Implantology***

Sébastien Granger — Xavier Pennec — Alexis Roche

N° 4169

Avril 2001

THÈME 3



*Rapport
de recherche*

Rigid Point-Surface Registration using Oriented Points and an EM Variant of ICP for Computer Guided Oral Implantology

Sébastien Granger^{*†}, Xavier Pennec^{*}, Alexis Roche^{*}

Thème 3 — Interaction homme-machine,
images, données, connaissances
Projet Epidaure

Rapport de recherche n° 4169 — Avril 2001 — 21 pages

Abstract: We investigate in this research report the rigid registration of a set of points with a surface for computer-guided oral implants surgery. We first formulate the Iterative Closest Point (ICP) algorithm as a Maximum Likelihood (ML) estimation of the transformation and the matches. Then, considering matches as a hidden random variable, we show that the ML estimation of the transformation alone leads to a criterion efficiently solved using an Expectation-Maximisation (EM) algorithm.

This algorithm implies a new parameter, based on the standard-deviation of the noise on points position. We demonstrate that, for small values, the algorithm behaves like the accurate ICP, while, for high values, the algorithm robustly aligns the barycenter and inertia moments. Finally, this parameter is decreased using an annealing scheme, which can be seen as a kind of multi-scale scheme. We present besides an efficient way to use oriented points - like surface points with their normals - instead of points with ICP and EM algorithms.

The experimental section provides evidences that the EM algorithm is far more robust and more accurate than ICP and reaches a global accuracy of 0.2 mm with computation times compatible with a per-operative system. Another important property is that the criterion analysis enables an easy distinction between correct results and false positives.

Key-words: medical imaging, rigid registration, ICP algorithm, EM algorithm

^{*} Epidaure

[†] CIFFRE Ph.D fellowship from AREALL, Neuilly-sur-Seine, France

Recalage rigide points orientés-surface : une variante de l'ICP fondée sur l'EM appliquée à l'implantologie dentaire robotisée

Résumé : Nous étudions ici le recalage rigide entre un nuage de points et une surface et l'appliquons dans le cadre d'un système de guidage per-opératoire pour l'implantologie dentaire. Nous montrons tout d'abord que l'algorithme ICP (Iterative Closest Point) peut-être considéré comme une Maximisation de la Vraisemblance (ML) de la transformation et des appariements. Nous appliquons alors les principes de l'algorithme EM (Expectation-Maximisation) en considérant les appariements comme une variable cachée.

L'algorithme ainsi introduit fait appel à un nouveau paramètre basé sur la variance du bruit. On démontre que l'algorithme se comporte comme le précis ICP lorsque ce paramètre est sous-estimé, et réaligne de façon robuste barycentres et tenseurs d'inertie lorsque ce paramètre est sur-estimé. Cette propriété remarquable suggère d'utiliser une approche multi-échelle, en l'occurrence de diminuer le paramètre en utilisant un recuit simulé. Nous présentons aussi une manière efficace d'utiliser les points orientés - comme les points d'une surface et leurs normales - avec l'ICP et l'EM.

Les expériences montrent que ce nouvel algorithme est plus précis et surtout beaucoup plus robuste que l'ICP. Sur nos données, la précision globale est de l'ordre de 0.2 mm, et le temps de calcul, quadruplé, reste compatible avec une application per-opératoire. Une autre propriété intéressante est que l'analyse du critère permet la discrimination entre résultats corrects et incorrects.

Mots-clés : imagerie médicale, recalage rigide, algorithme ICP, algorithme EM

Contents

1	Introduction	4
1.1	Registration of two sets of points: ICP and variants	4
1.2	Report organisation	6
2	Maximum likelihood estimations of the transformation: ICP and EM algorithms	6
2.1	Maximum Likelihood and standard ICP	7
2.2	Maximum likelihood with uncertain matches	8
2.3	From the Maximum likelihood to the EM criterion	9
2.3.1	Designing the auxiliary criterion	9
2.3.2	E-Step: estimation of matches	9
2.3.3	M-Step: registration	10
3	Practical use of the EM algorithm	10
3.1	Mahalanobis distance: the case of oriented points	10
3.2	Setting the variance parameter: direct estimation and deterministic annealing	11
3.3	Convergence	12
3.4	Final algorithm implementation	12
4	Experiments and discussion	13
4.1	Robustness and Internal Accuracy	13
4.2	External accuracy	15
4.3	Global accuracy	16
4.4	Registration Time	16
5	Conclusion	17
6	Acknowledgements	17
7	Appendix	19
7.1	EM limit for a low variance	19
7.2	EM limit for a high variance	19
7.2.1	Translation part	19
7.2.2	Rotation part	20

1 Introduction

Oral implantology is a domain where computer guided surgery can lead to drastic improvements in safety and quality of the operation for the patient. The operation is planned on a pre-operative CT-Scan and the purpose of such a system is to help the dentist to drill the implant in the predefined position and orientation. *Pre-operative systems* are designed to construct a surgical guide (a jaw splint), today constructed by hand. These are the most simple systems, since the robotic phase take place before the operation, but are less accurate and are not suited in a significant number of cases, because they obstruct the mouth. *Per operative systems* are based on a real-time guiding. They are more versatile and accurate, but have to comply with per-operative constraints such as computation time, minimal interactivity, patient movements... All these systems include a rigid registration step to put into correspondence the robot and the planning image coordinate systems. Extrinsic registration methods are based on artificial landmarks, easy to match and register, but usually not very numerous and accurate. Intrinsic methods are usually based on curves and surfaces extracted from images or sampled on the anatomical object to register. Since there is more information, the resulting transformation is more accurate.

The *DentalNavigator* system (patent pending), developed by AREALL [6], is a per-operative system based on surface registration. In the CT-Scan image, the teeth and jaw bone surfaces are easily segmented using a Marching-Cube algorithm resulting in about 100000 oriented and triangulated points. Points on the same structures are measured in the patient coordinate system using an ultrasound sensor mounted on a passive robotic arm. This time we get between 50 and 1000 unstructured points with rough normal estimations. After the registration, the US sensor is replaced by the drill on the robot arm and the system visually guides the surgeon to the planned position and orientation for drilling. In this article, we investigate the registration step of this system.

1.1 Registration of two sets of points: ICP and variants

The registration of two (structured or unstructured) set of points is usually performed using one of the multiple variations around the Iterative Closest Point algorithm [10, 17]. The basic idea is to minimise the average distance from each point s_i of the scene to its closest point m_j in the transformed model. Given these matches, one can compute the transformation and iterate. Thus, one minimises the criterion:

$$C(T) = \sum_i \min_j \|s_i - T \star m_j\|^2 \quad (1)$$

As no closed-form method exists, one introduces a secondary criterion based on an explicit representation of matches, which is alternatively minimised w.r.t. the matches (the two criterions are then equal) and the transformation.

Many variants and improvements of this algorithm have been proposed since:

Distance function and feature type : The ICP criterion is based on the euclidian distance between points. It can easily be adapted by changing the distance function and the feature type. For instance, in [15], Mahalanobis distance is used to take heteroscedastic (non isotropic, non-homogeneous) noise into account, and is demonstrated with points and frames. The main improvement is on the robustness, since matches are much easier to determine.

Optimisation methods : The matching estimation step can be done efficiently using a kD-tree or other space-partitioning methods. For the estimation of the rigid transformation, there exists four closed-form solutions when features are points, with similar efficiency and accuracy [7]. With other types of features, no closed-form is known and one has to lean on iterative methods such as gradient descent or Kalman filtering. Kanatani [9] proposed to apply his renormalisation theory to rotation estimation, and [3] derived it for rigid transformations.

Outliers and robustness problems : Since the errors are squared, the transformation computation is very sensible to false positives (erroneous matches). The influence of such outliers can be cancelled (or at least limited) using robust estimators [11]: M-estimators based e.g. on a simple truncated distance function [17, 15], or S-estimators such as the minimizer of the Least Median of Squares (LMS) [13].

Accuracy evaluation : Under certain hypotheses on the noise, the algorithm is optimal and one could evaluate its theoretical accuracy by evaluating the consequences of the noise model on the transformation evaluation: Kanatani [9] presented it as a Cramer-Rao lower bound, and Pennec [15] derived it using its statistical framework on rotations and rigid transformations. The accuracy is also directly computed when using a Kalman filter, or can be evaluated using computer intensive bootstrap methods [3].

Point matching strategy : The original closest-point strategy lacks flexibility, since each scene point can be matched with only one model point with an implicit constant weight. Moreover, sudden changes in closest-point detection lead to a highly non-convex energy function, full of local minima. A first improvement consists in using a non-uniform weight, computed using extra reliability information. A second improvement consists in using multiple weighted matches for each scene point. Rangarajan et al. have studied some of these methods, always based on an energy function in order to preserve the convergence properties of the alternated minimisation. They introduced a probabilistic vision of the matching problem, and developed models based on Gaussian weight (SoftAssign [1]) and Mutual Information [2]. All these models are based on a smooth point-matching estimation, so that the energy function is smoother than in the standard ICP. This implies a smaller number of local minima and thus a better accuracy and robustness.

Extension to surface registration : Though ICP is often presented as a surface-based registration algorithm, all previous variants are point-based methods in the sense that they assume one-to-one correspondences between model and scene points. There are no such correspondences in surfaces sampled in two different ways. Chen and Medioni [16] proposed to use a more surface specific method relying on a first-order approximation of the surface, i.e. the tangent plane defined by the closest model point and its normal.

1.2 Report organisation

Starting from ICP, our main motivation was to improve the accuracy and the robustness in view of a real time system. The previous review suggested two main ideas.

Firstly, we experimentally observed that Rangarajan’s algorithms [1, 2] were only efficient for registering two comparable sets of points (e.g. landmarks or surface equally sampled). Another problem is that there is an implicit dependence assumption between the scene points. This implies the storage of all weights for subsequent complex and time consuming “renormalisations”. Our problem is slightly different because the per-operative set of points is highly sub-sampled compared to the segmented surface. Thus, scene points are sparse enough to be considered as independent measures of unknown model points. Following Rangarajan’s probabilistic approach, we consider our registration as an incomplete data problem and develop in section 2 a new registration criterion based on Expectation-Maximisation principles. A similar criterion, inspired from [14], was independently developed in [8], but the design of our algorithm is original. In section 3, we demonstrate new important properties leading to an efficient implementation of the algorithm. Finally, we discuss in section 4 the experimental results on our oral implantology application in terms of robustness, internal, external and global accuracy.

Secondly, normals are available in our case for the scene and the model. Thus, it seems logical to use a *distance between oriented points* in order to increase the quality of the matches. We present in section 3.1 such a distance which is compliant with closed-form optimisation methods, so that algorithm speed is not penalised.

2 Maximum likelihood estimations of the transformation: ICP and EM algorithms

In this section, we model the scene as a random process, and we show that a maximum likelihood estimation of the transformation and the matches leads to the ICP algorithm using the Mahalanobis distance. Then considering matches as a secondary random process of no interest, we maximise the likelihood of the scene knowing only the transformation. Finally, we show how to solve efficiently this last criterion using an EM algorithm.

For the sake of simplicity, we use an isotropic and homogeneous noise (though other cases can be handled with Mahalanobis distance), and we do not address here the problem of outliers, but the framework can be easily extended to that case by adding a probability to match a scene feature to the background [14, pp.78].

2.1 Maximum Likelihood and standard ICP

Let s_i be the features of the scene \mathcal{S} , m_j the features of the model \mathcal{M} , μ^2 the Mahalanobis distance between features and T a rigid transformation from the model to the scene. In this section, we compute the likelihood of the scene assuming a Gaussian noise on the scene and exact matches and transformation. Looking for the matches and the transformation that maximises this likelihood will lead to the ICP algorithm.

Assuming that s_i is homologous to m_j , i.e. a measure of $T \star m_j$ corrupted with an additive Gaussian noise, its density probability function is:

$$p(s_i|m_j, T) = k^{-1} \cdot \exp\left(-\frac{\mu^2(s_i, T \star m_j)}{2}\right) \quad (2)$$

where k is the normalisation constant.

Because we deal later on with multiple and weighted matches, we use a matrix A to represent matches estimation where $A_{ij} = 1$ if s_i matches m_j and 0 otherwise. Since each scene point s_i is assumed to correspond exactly to one model point with index say $\pi(i)$, we have $A_{ij} = \delta_{j\pi(i)}$ and $\sum_j A_{ij} = 1$ for all scene index i . As $\alpha^\beta = \alpha$ if $\beta = 1$ and 1 if $\beta = 0$, we can write the conditional pdf of s_i knowing the whole model, the matches and the transformation as: $p(s_i|A, \mathcal{M}, T) = \prod_j (p(s_i|m_j, T))^{A_{ij}} = p(s_i|m_{\pi(i)}, T)$.

Assuming now that all scene points are conditionally independent, the scene likelihood is then the product of each scene point pdf:

$$p(\mathcal{S}|A, \mathcal{M}, T) = \prod_{ij} (p(s_i|m_j, T))^{A_{ij}} \quad (3)$$

Taking the negative log, we obtain the following criterion to be maximised:

$$C(T, A) = -\sum_{ij} A_{ij} \cdot \log p(s_i|m_j, T) = \sum_{ij} A_{ij} \cdot \frac{\mu^2(s_i, T \star m_j)}{2} + \sum_{ij} A_{ij} \cdot \log k$$

As k is constant, and A checks $\sum_j A_{ij} = 1$, this simplifies into:

$$C(T, A) = \frac{1}{2} \sum_{ij} A_{ij} \cdot \mu^2(s_i, T \star m_j) + n_{\mathcal{S}} \cdot \log k$$

One recognises here the standard ICP criterion using the Mahalanobis distance, up to an additive constant. This proves that ICP maximises the scene likelihood under a Gaussian noise with exact correspondences. Moreover, [9] showed that this is the best (minimal variance) estimator. One can also relate this result to the MAP estimation of [14] where the purpose is to maximise $p(A, T|\mathcal{S}) = p(\mathcal{S}|A, T) \cdot p(A, T) / p(\mathcal{S})$. As $p(\mathcal{S})$ is constant and the matches and the transformation are assumed to be independent, this simplifies into $p(A, T|\mathcal{S}) = \alpha \cdot p(\mathcal{S}|A, T) \cdot p(A) \cdot p(T)$. When assuming uniform priors on the matches and the transformation, the two approaches are equivalent.

Here, the criterion is invariant w.r.t a global scaling of the noise variance. This property will not hold for the following EM formulation.

2.2 Maximum likelihood with uncertain matches

In the previous section, the transformation and the matches were both estimated by directly maximising the scene likelihood knowing these variables. In fact, we only need to determine the transformation for our application, and the matching matrix is an auxiliary variable. Moreover, there can be ambiguities in the matching estimation with almost equal scene likelihoods. Thus, one idea is to take into account these multiple possible matches in the criterion weighted by their a-posteriori probability. Another idea is to look for *the transformation that maximises the likelihood of the scene knowing only the transformation*. These two approaches are in fact equivalent and efficiently resolved with EM algorithm.

Another way to see the multiple matches is to remember that the model is a surface: let us take for instance a scene point s near a face of this triangulated surface. Its homologous point m is somewhere on the triangle. Allowing to multiply match s to the three vertices m_i with some probabilities π_i in the ICP criterion amounts to match s to the virtual point $m = \frac{1}{\pi_1 + \pi_2 + \pi_3}(\pi_1 \cdot m_1 + \pi_2 \cdot m_2 + \pi_3 \cdot m_3)$, which can now be any point of the triangle. Taking the weights as a decreasing function of the distance from s to each vertex can be viewed as (and will be compared to) an approximation of the projection onto the surface.

Consider now a random matching matrix \mathbf{A} . Each possible matching matrix A has a probability $p(A) = P(\mathbf{A} = A)$ and verifies the constraints of the previous section. Since A_{ij} has binary values, we have $\overline{A_{ij}} = E(\mathbf{A}_{ij}) = P(\mathbf{A}_{ij} = 1) \in [0, 1]$. The row constraint (each scene point has only one corresponding model point) translates into $\sum_j \overline{A_{ij}} = 1$. Finally, since scene points are assumed to be independent, the matrix rows are independent, so that

$$p(A) = \prod_{ij/A_{ij}=1} p(\mathbf{A}_{ij} = 1) = \prod_{ij} (\overline{A_{ij}})^{A_{ij}} \quad (4)$$

Let us start from an a-priori probability law given by $p(A) = \prod_{ij} (\overline{\pi_{ij}})^{A_{ij}}$ (since we only know the model and not the scene, a relevant choice is the uniform law $\overline{\pi_{ij}} = \frac{1}{n_{\mathcal{M}}}$). Using Bayes rule and Eq. 3, we can deduce the joint scene and matching matrix likelihood:

$$p(\mathcal{S}, A | \mathcal{M}, T) = p(\mathcal{S} | A, \mathcal{M}, T) \cdot P(A | \mathcal{M}, T) = \prod_{ij} (\overline{\pi_{ij}} \cdot p(s_i | m_j, T))^{A_{ij}} \quad (5)$$

Thus, *the likelihood of the scene knowing only the transformation is:*

$$p(\mathcal{S} | \mathcal{M}, T) = \sum_{\{A\}} p(\mathcal{S}, A | \mathcal{M}, T) = \prod_i \left(\sum_k \overline{\pi_{ik}} \cdot p(s_i | m_k, T) \right) \quad (6)$$

Taking the negative log, we obtain the registration criterion:

$$C(T) = -\log(p(\mathcal{S} | \mathcal{M}, T)) = -\sum_i \log \left(\sum_k \overline{\pi_{ik}} \cdot p(s_i | m_k, T) \right) \quad (7)$$

2.3 From the Maximum likelihood to the EM criterion

This criterion, like the first ICP criterion (Eq. 1), has no closed-form solution. We construct in this section an auxiliary criterion, depending explicitly on the matching matrix, and we use an alternated optimisation scheme. This construction follows EM principles [4, 12] and the auxiliary variables framework of [5].

2.3.1 Designing the auxiliary criterion

For any matching matrix A , we can write the criterion using Bayes rule: $C(T) = -\log p(A, \mathcal{S}|\mathcal{M}, T) + \log p(A|\mathcal{S}, \mathcal{M}, T)$, where $p(A|\mathcal{S}, \mathcal{M}, T)$ is the a-posteriori likelihood of matches. Since this is valid for any matching matrix A , it is still for the expectation w.r.t. *any* random matching matrix \mathbf{A} :

$$C(T) = -E_{\mathbf{A}}(\log p(A, \mathcal{S}|\mathcal{M}, T)) + E_{\mathbf{A}}(\log p(A|\mathcal{S}, \mathcal{M}, T))$$

To introduce an explicit dependence on the matching matrix, let us add to this criterion the Kullback-Leibler distance $E_{\mathbf{A}}\left(\log \frac{p(A)}{p(A|\mathcal{S}, \mathcal{M}, T)}\right)$ between the random variable \mathbf{A} and the random variable \mathbf{A}_T defined by the a-posteriori likelihood of matches: $p(\mathbf{A}_T = A) = p(A|\mathcal{S}, \mathcal{M}, T)$. This distance is positive and of course null (thus minimised) for $\mathbf{A} = \mathbf{A}_T$. Thus, we have:

$$C(T, \mathbf{A}) = -E_{\mathbf{A}}(\log p(A, \mathcal{S}|\mathcal{M}, T)) + E_{\mathbf{A}}(\log p(A)) \quad (8)$$

with $C(T) = \min_{\mathbf{A}} C(T, \mathbf{A}) = C(T, \mathbf{A}_T)$. An efficient optimisation scheme for this new criterion is then to alternate an Expectation step to estimate the matching matrix and a Minimisation step to optimise for the transformation.

2.3.2 E-Step: estimation of matches

In this step, we want to compute the optimal values $\overline{A_{ij}}$. By definition of our auxiliary criterion, the optimal \mathbf{A} has the pdf:

$$p(A_T) = p(A|\mathcal{S}, \mathcal{M}, T) = \frac{p(A, \mathcal{S}|\mathcal{M}, T)}{p(\mathcal{S}|\mathcal{M}, T)} = \prod_{ij} \left(\frac{\overline{\pi_{ij}} \cdot p(s_i|m_j, T)}{\sum_k \overline{\pi_{ik}} \cdot p(s_i|m_k, T)} \right)^{A_{ij}}$$

Since we have $p(A_T) = \prod_{ij} (\overline{(A_T)_{ij}})^{A_{ij}}$, we obtain by identification:

$$\overline{(A_T)_{ij}} = \frac{\overline{\pi_{ij}} \cdot p(s_i|m_j, T)}{\sum_k \overline{\pi_{ik}} \cdot p(s_i|m_k, T)} = \frac{\overline{\pi_{ij}} \cdot \exp(-\mu^2(s_i, T \star m_j)/2)}{\sum_k \overline{\pi_{ik}} \cdot \exp(-\mu^2(s_i, T \star m_k)/2)} \quad (9)$$

Contrary to the ICP (see remark at end of 2.1), these values are not invariant w.r.t a global scaling of the noise variance. Hence, the noise variance is an effective parameter of the EM algorithm (see section 3).

2.3.3 M-Step: registration

Now that we have an estimation of the matching matrix, we can optimise the criterion for the transformation. In Eq. 8, only the first term depends on the transformation: we have to minimise $-E_{\mathbf{A}}(\log p(A, S|\mathcal{M}, T)) = -\sum_{ij} \overline{A_{ij}} \log(\overline{\pi_{ij}} \cdot p(s_i|m_j, T))$. Discarding constant and normalisation factors, we are left with the minimisation of:

$$\sum_{ij} \overline{A_{ij}} \cdot \frac{\mu^2(s_i, T \star m_j)}{2} = \sum_{ij} \overline{A_{ij}} \cdot \frac{\|s_i - T \star m_j\|^2}{2 \cdot \sigma_s^2} \quad (10)$$

Actually, this is the *expectation of the standard ICP algorithm w.r.t. the random matching matrix*, as suggested in the beginning of section 2.2.

For the practical implementation of the minimisation algorithm, the only differences with the ICP criterion are the non-binary weights. In the rigid case, this leads to a straightforward adaptation of the SVD or the unit quaternion methods [7].

3 Practical use of the EM algorithm

In this section, we first present the Mahalanobis distance for oriented points. Then, we analyse the role of the variance parameter and its influence on the criterion shape. We investigate different technics to chose this parameter and the impact on the convergence of the algorithm. We end up with the pseudo-code of the algorithm.

3.1 Mahalanobis distance: the case of oriented points

The Mahalanobis distance is usually used in statistics to take the noise covariances into account, for instance in heteroscedastic (non uniform, non isotropic) systems. For example, with oriented-points the covariance on the point position and the normal orientation are not comparable. We present in the sequel a rigorous definition of the Mahalanobis distance between oriented-points and give an approximation well suited to the closed-form optimisation methods used in ICP.

Firstly, notice that the Mahalanobis distance between two couples of independent variables is the sum of the Mahalanobis distances between each independent variable. Thus, if we assume that *the point position and the normal orientation are independent*, the Mahalanobis distance is simply $\mu^2((x, n_x), (y, n_y)) = \mu^2(x, y) + \mu^2(n_x, n_y)$. [15] discussed the rigorous definition of the Mahalanobis distance in non-vectorial manifolds. For normals, in the *isotropic case*, $\mu^2(n_x, n_y)$ is simply $(\widehat{n_x, n_y})^2 / \sigma_{n_x}^2$, where σ_{n_x} is the standard deviation of the angle between normals. Thus, in the isotropic and independent case, we end-up with: $\mu^2((x, n_x), (y, n_y)) = \|x - y\|^2 / \sigma_x^2 + (\widehat{n_x, n_y})^2 / \sigma_{n_x}^2$.

Unfortunately, when using this distance with ICP, there is no closed-form method for the transformation re-estimation. However, for small normal differences, a Taylor expansion of the difference of the normal unit vectors w.r.t. $\theta = (\widehat{n_x, n_y})$ gives $\|n_x - n_y\| = 2 \cdot |\sin(\theta/2)| =$

$\theta + O(\theta^3)$. This approximation is moreover a robust M-estimator of the distance. Finally, our practical Mahalanobis distance between oriented points is:

$$\mu^2((x, n_x), (y, n_y)) \simeq \|x - y\|^2 / \sigma_x^2 + \|n_x - n_y\|^2 / \sigma_{n_x}^2$$

Thus, our registration criterion (Eq. 10) can be written as:

$$\sum_{ij} \overline{A_{ij}} \cdot \frac{\mu^2(s_i, T \star m_j)}{2} = \sum_{ij} \overline{A_{ij}} \cdot \left(\frac{\|s_i - T \star m_j\|^2}{2 \cdot \sigma_s^2} + \frac{\|n_{s_i} - T \star n_{m_k}\|^2}{2 \cdot \sigma_{n_s}^2} \right) \quad (11)$$

In this formula, normals are treated as standard vectors, thus leading to a straightforward adaptation of the closed-form methods for the rotation estimation (the translation does not explicitly depend on the normals).

3.2 Setting the variance parameter: direct estimation and deterministic annealing

To analyse the role of the variance, let us see first how the criterion behaves for asymptotic values of this parameter. If the variance goes to zero, it is easy to show (see annex 7.1) that the limit of equation 9 is: $\overline{(A_T)}_{ij} = 1$ for the closest point and 0 otherwise. Thus, the ICP algorithm is the limit of the EM algorithm for very small variance parameter.

On the contrary, when the variance goes to infinity, the EM algorithm aligns barycentre and inertia moments (see annex 7.2 for a proof), generally leading to a shifted result (see Fig. 1).

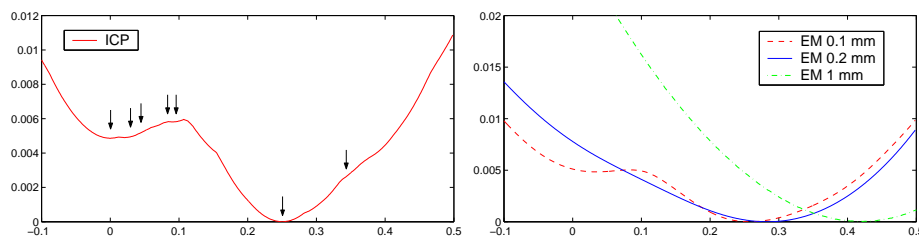


Figure 1: *Criterion vs Z-translation for ICP (on the left) and for EM with various variances (on the right)*. There are two relevant minima for ICP (0, where the algorithm stopped, and 0.25, where criterion is minimum) and two irrelevant ones (0.1 and 0.3), where the algorithm could stop with appropriate initialisation. The EM algorithm has a much smoother shape. In this case, the noise of the point position was estimated to 0.18 mm while the mean distance between neighbouring model points is 0.2 mm. For an under-estimated variance (0.1 mm) the irrelevant minima have disappeared. For the approximative noise variance (0.2 mm), even the first minima has disappeared. For a larger (overestimated) variance (1 mm), the criterion is almost quadratic, but the global minimum has clearly been shifted.

Since under-estimating the variance leads to less accurate results (see experimental results in section 4.3) while over-estimating it suppress irrelevant minima, it is logical to start with a large variance (e.g. ten time greater than expected), and decrease it to reach the real noise variance. This approach is a kind of multi-scale strategies.

One could think to directly compute the variance after each step of the EM algorithm from the estimated weights and transformation: considering the variance as an additional parameter and optimising for it at fixed transformation and weights leads to:

$$\sigma_s^2 = \frac{\sum_{ij} \overline{A_{ij}} \cdot \|s_i - T \star m_j\|^2}{dim \cdot N_S} \quad \sigma_{n_s}^2 = \frac{\sum_{ij} \overline{A_{ij}} \cdot \|n_{s_i} - T \star n_{m_j}\|^2}{(dim - 1) \cdot N_S} \quad (12)$$

Experiments showed that this estimation is not robust because the decrease is too fast: the algorithm cannot escape the local minima. A slight and regular decrease facilitates the convergence to the global minimum. This can be realised using a deterministic annealing [1] where the variance is multiplied by an annealing coefficient (usually between 0.9 and 0.95) after each iteration, until the real noise variance has been reached. This technique allows to avoid local minima to finally reach a very accurate result, but requires a good estimation of the noise variance.

3.3 Convergence

Since ICP and EM minimise a global criterion alternatively along subsets of the parameters, the criterion always decrease and convergence to a local minimum is ensured. In practice, the algorithm is stopped when the variations of the parameters are small (threshold on the residual transformation). However, the annealing scheme on the variance is not a minimisation step. Thus, the convergence of the algorithm should only be tested after the end of the annealing, when the variance is minimal.

3.4 Final algorithm implementation

For the experiments, we used the following algorithm setup: an annealing coefficient $\alpha = 0.9$ with initial variances equal to 10 times the real point and orientation noise variances σ_r^2 and $\sigma_{n_r}^2$ and a simple outlier rejection using a threshold on the Mahalanobis distance at $\mu_{max}^2 = 3 \cdot dim$. The estimation of the real variance was performed once on a reliable dataset (using equation 12), and used for other similar datasets.

Initialisation : Compute T_0 , set $\sigma_s^2 = 10 \cdot \sigma_r^2$, $\sigma_{n_s}^2 = 10 \cdot \sigma_{n_r}^2$.

Repeat E-Step : For each s_i :

Search all m_j such that $\|s_i - T_t \star m_j\|^2 < \sigma_s^2 \cdot \mu_{max}^2$ using a kD-Tree

Compute the distances $\mu^2((s_i, n_{s_i}), T_t \star (m_j, n_{m_j}))$

Compute the weights $(\overline{A_{T_t}})_{ij}$ using Eq. 9

Compute the criterion value $C(T_t) = C(T_t, \mathbf{A}_{T_t})$ using Eq. 7

M-Step : Compute the transformation T_{t+1} minimising Eq. 11.

Annealing : Set $\sigma_s^2 = \max(\alpha \cdot \sigma_s^2, \sigma_r^2)$, $\sigma_{n_s}^2 = \max(\alpha \cdot \sigma_{n_s}^2, \sigma_{n_r}^2)$.

Until $\sigma_s^2 = \sigma_r^2$ and $\{d(T_t, T_{t+1}) < \varepsilon \text{ or } C(T_{t+1}) \geq C(T_t)\}$

4 Experiments and discussion

We evaluate in this section the comparative robustness and accuracy of the ICP and EM algorithms on our data. For the robustness, we estimate the size of the basin of convergence where an initial transformation leads to the correct global minimum. For the accuracy, we have to distinguish between the following three main types of errors.

- *Internal accuracy*: for same data, several good results can be reached, depending on the initialisation. This can be interpreted as the consequence of errors in the matching matrix estimation, and introduce a first source of accuracy.
- *External accuracy*: even with a perfect estimation of the matching matrix, the noise on the data introduces a second source of inaccuracy.
- *Surface accuracy*: all algorithms described here are point-based algorithm: we assume that each scene point match one model point. This hypothesis is only valid for landmarks registration, and not for surface registration. Though algorithms work well with surfaces too, this introduces a third source of inaccuracy.

In these experiments, no ground truth was available (or was far less accurate than algorithm, so that results would not have been reliable). Thus we decided to use a statistical comparison of experimental results: for each experiment, several registrations were made with the model and the scene in same positions, and the covariance of the resulting transformations around their mean was computed using [15] (Roughly, transformations are centred around identity, and converted into a vectorial representation such as translation and rotation vector. Mean and covariance are then computed in this representation). This covariance is difficult to discuss, but can be used to deduce the mean standard deviation of points in an area of interest. This is indeed what is done here taking the whole jaw as the area of interest. This gives a pretty good idea of the algorithm accuracy, though it does not take into account a possible systematic bias.

Notice that the normal orientation is not very precise on scene points (the standard deviation is about 25 degrees), so that the improvements are not very spectacular.

4.1 Robustness and Internal Accuracy

The robustness can be characterised by the size of the attraction basin of the global minimum. However, even if the algorithm converges towards the global minimum, it may be trapped in some small local minima in its immediate vicinity due to errors in the matches

estimation. We call *internal accuracy* this intrinsic variability of the results. The problem is to choose a limit that distinguishes between internal accuracy errors and “uniformly distributed” erroneous convergences outside the attraction basin.

In this experiment, we used a surface segmented from a CT-Scan and a set of 50 points measured on the real jaw. We perturbed 2000 times the results of an “exact” registration by adding uniform translations up to 2 cm (*on these data*, we observed that both algorithms were almost insensitive to rotations up to 10 degrees), used it as initialisation of the ICP and EM algorithms and plot in figure 2 (top) the distance of the estimated to the “exact” transformation. For ICP, (upper left), we observe many local minima, and it is difficult to differentiate a clear structure around 0 from a uniform distribution elsewhere. As rotation and translation are well correlated under 1 mm and 1 deg, we arbitrarily decided that these transformations were representative of the internal accuracy. For the EM algorithm (upper right), the number of local minima has significantly decreased and there is a clear separation between transformations very close to zero and other local minima. Propagating the transformation covariance on test points in the area of interest (the jaw) gives us a measure of the internal accuracy: 0.2 mm for ICP, and 0.007 mm for EM.

Now, to determine the size of the attraction basin, we have to look for the smallest initial translation for which the result is classified as bad. We plot in Fig. 2 (bottom left) the percentage of convergence to the global minimum w.r.t. the initial transformation: an initial translation of 2 mm can lead to bad results with ICP, whereas this limit is shifted to 9 mm for the EM. Last but not least, we present in Fig. 2 (bottom right) the distributions of the criterion values for both algorithms: there is a clear threshold distinguishing good from bad results with EM, whereas there is no such clustering for ICP. Other experiments

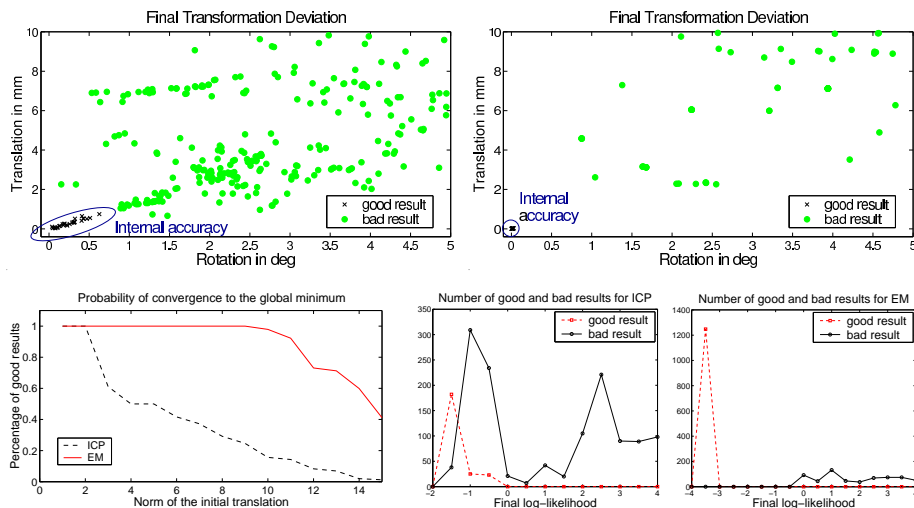


Figure 2: **Top:** Final transformations distribution for ICP (on the left) and EM (right). **Bottom:** probability of convergence to the global minimum with respect to the norm of the initial translation (left), and distribution of the criterion value (right).

showed that this threshold on EM strongly depends on the noise variance but only slightly on the data shape. Thus, it can be estimated only once for a given application.

Figure 3 present experimental results with EM algorithm enhanced by the use of normals. The general structure of the results is the same, though we can observe small improvements: the number of local minima has decreased, and the algorithm correctly converges in a slightly wider area.

4.2 External accuracy

The external inaccuracy is defined as the consequence of noise on features position. Here it is experimentally measured, though it can be evaluated theoretically. All algorithms provide comparable results.

The scene and model features are of course not exact. In our case, the CT-Scan noise and the segmentation algorithm introduce errors in model features, and scene features are measured with a robotic arm, which precision is limited. In order to simplify, *we report the model noise on the scene features, and consider the model as exact*. For fixed matches, the registration result is subject to variations due to the noise on the features position. Only this type of accuracy can be evaluated theoretically: indeed, the methods presented in [9, 15, 3] do not take into account errors in the matches estimation.

In our experiments, we saved the matching matrix after a good registration, and realised 1000 other registrations with the same matching matrix and model, but after having applied a Gaussian noise on scene points. We used a variance of 0.35 mm on the point position, which is roughly the amount of noise on our data. Results for ICP and EM are comparable, inducing a variability of 0.13 mm in our area of interest.

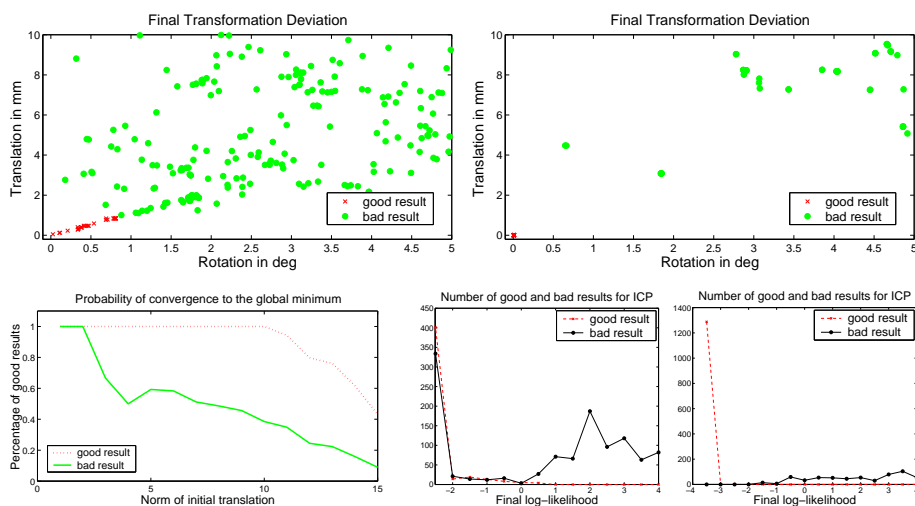


Figure 3: **Top:** *Final transformations distribution for ICP (on the left) and EM (right) with normals.* **Bottom:** *probability of convergence to the global minimum with respect to the norm of the initial translation (left), and distribution of the criterion value (right).*

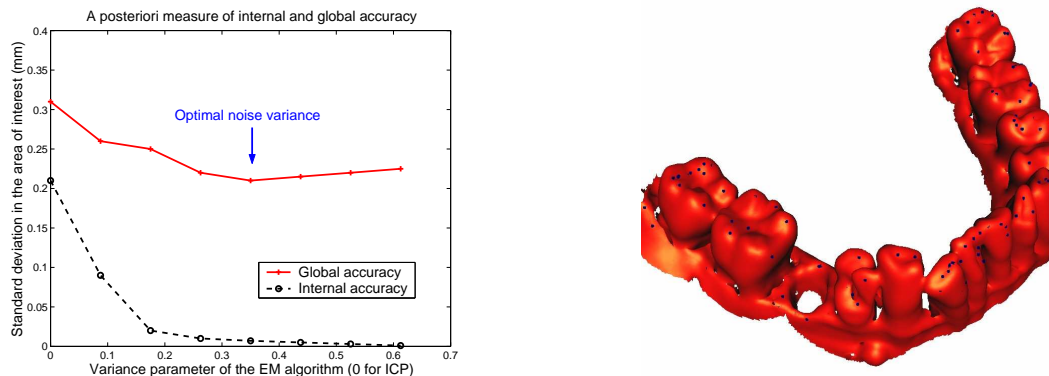


Figure 4: **Left:** *global and internal accuracy of the EM with respect to the variance. ICP (at $\sigma = 0$) exhibits internal and global accuracies of 0.22 mm and 0.31 mm, while EM presents at the optimal variance internal and global accuracies of 0.007 mm and 0.22 mm. Right:* *A view a the points-surface registration for the optimal variance.*

Other experiments proved that results when using normals are not significantly different. For instance, adding an important orientation noise (about 25 degrees) introduces an extra inaccuracy of about 0.002 mm. This proves that, if normals can increase robustness, they don't play an important role in terms of accuracy.

4.3 Global accuracy

To evaluate the global accuracy (i.e. the difference between the “exact” and estimated transformation) of the algorithms in real conditions, ten sets of scene points were acquired in the same position and registered onto the same model. Thus, the model variability was not taken into account, but all other sources of errors (CT-Scan segmentation error, scene points measurement error, and especially effect of surface sampling) were realistic. The “exact” registration was determined by the registration of all sets of points together to the model surface: this transformation should have a variance 10 times smaller than individual registrations, but hides a possible bias. Figure 4 presents the standard deviation of test points on the jaw for different values of the variance in the EM algorithm: underestimating this parameter appears to be much more penalising in terms of accuracy than overestimating it.

4.4 Registration Time

In the scope of a per-operative system, the computation time is a key parameter. In both algorithms, this time depends strongly on the number of scene points and iterations, and the distance threshold. Thanks to efficient space-partitioning structures, it only slightly depends on the number of model points. For each iteration (with the same data and distance threshold), EM only adds a 30% overhead to the ICP time, but it usually needs much more iterations to converge. Typically, it took 50 iterations (including 20 for deterministic

annealing) on the above experiment, against 20 for ICP. The final time comparison is four to one in favour of ICP. However, the total computation time of EM is about 30 s in our case, which is still reasonable for our per-operative system. Note that using normals don't penalise the computation time.

5 Conclusion

We present in this article a maximum likelihood approach of the point matching problem and show that looking for both the transformation and the matches leads to the ICP algorithm, while considering the matches as hidden variables gives a new criterion, efficiently solved using an EM method. In this new algorithm, the variance on the data points is an important parameter that allow the EM algorithm to range from a global (alignment of the barycentres and inertia tensors) to a purely local behaviour (ICP). This property is exploited in a deterministic annealing method to avoid local minima while reaching an optimal accuracy.

Experimental results show that ICP has a very small attraction basin (a few millimetres in translation), an important internal error and a global accuracy of 0.31 mm in the jaw area. The EM algorithm exhibits a much wider attraction basin (around 1 cm) with a negligible internal error and a better global accuracy (0.22 mm). This gain in robustness and accuracy is counterbalanced by a larger computation time (a factor 4), which remains however compatible with our per-operative system.

Future work will include the parallelisation of the algorithm, the study of the surface sampling influence on the accuracy, more experiments about the the use of oriented points and the online prediction of the registration uncertainty.

6 Acknowledgements

This work was supported by a CIFFRE Ph.D fellowship from AREALL, who also provided all the data used in this study.

References

- [1] A. Rangarajan and al. A Robust Point-Matching Algorithm for Autoradiograph Alignment. *Medical Image Analysis*, 1(4):379–398, 1997.
- [2] A. Rangarajan, H. Chui and J.S. Duncan. Rigid Point Feature Registration Using Mutual Information. *Medical Image Analysis*, 3(4):425–440, 1999.
- [3] B. Matei and P. Meer. Optimal rigid motion estimation and performance evaluation with bootstrap. In *Proc. IEEE Conf. on Computer Vision and Pattern Recognition (CVPR'99)*, volume 1, pages 339–345, 1999.

-
- [4] C. Couvreur. The EM Algorithm: A Guided Tour. In *Proc. 2d IEEE European Workshop on Computationaly Intensive Methods in Control and Signal Processing (CMP'96)*, pages 115–120, Pragues, Czech Republik, August 1996.
 - [5] L. Cohen. Auxiliary variables and two-step iterative algorithms in computer vision problems. *J. of Mathematical Imaging and Vision (JMIV)*, (6):59–83, 1996.
 - [6] D. Etienne and al. A new approach for dental implant aided surgery. A pilot evaluation. In *Proc. CARS'2000*, pages 927–931, 2000.
 - [7] D.W. Eggert, A. Lorusso and R.B. Fisher. Estimating 3-D rigid body transformations : A comparison of four major algorithms. *Machine Vision and Applications*, 9:272–290, 1997.
 - [8] H. Chui and A. Rangarajan. A feature registration framework using mixture models. In *Proc. MMBIA'2000*, pages 190–197, 2000.
 - [9] K. Kanatani. *Statistical Optimization for Geometric Computation : Theory and Practice*. Elsevier Science (Amsterdam), 1996.
 - [10] P.J. Besl and N.D. McKay. A Method for Registration of 3D shapes. *IEEE transactions on pattern analysis and machine intelligence*, 14(2):239–256, 1992.
 - [11] P.J. Rousseeuw and A.M. Leroy. *Robust regression and outlier detection*. Ed. John Wiley and Sons, 1987.
 - [12] R. M. Neal and G. E. Hinton. A view of the EM algorithm that justifies incremental, sparse, and other variants. *Learning in Graphical Models*, 1998.
 - [13] T. Masuda, K. Sakaue, and N. Yokoya. Registration and integration of multiple range images for 3D model construction. In *Proc. ICPR'96*, pages 879–883, 1996.
 - [14] W. Wells. Statistical approaches to feature-based object recognition. *Int. Journal of Computer Vision*, 21(1):63–98, 1997.
 - [15] X. Pennec and J.P. Thirion. A Framework for Uncertainty and Validation of 3D Registration Methods based on Points and Frames. *Int. Journal of Computer Vision*, 25(3):203–229, 1997.
 - [16] Y. Chen and G. Medioni. Object Modelling by Registration of Multiple Range Images. *Image and Vision Computing*, 10:145–155, 1992.
 - [17] Z. Zhang. Iterative Point Matching for Registration of Free-Form Surfaces. *Int. Journal of Computer Vision*, 13(2):119–152, 1994.

7 Appendix

7.1 EM limit for a low variance

Here is the proof that the EM algorithm behaves like standard ICP for a low variance. We can rewrite Eq. 9 as:

$$\overline{(A_T)_{ij}} = \frac{1}{1 + \sum_{k \neq j} \frac{\overline{\pi_{ik}}}{\overline{\pi_{ij}}} \cdot r_{ijk}} \quad \text{with} \quad r_{ijk} = \exp\left(\frac{d^2(s_i, T \star m_j) - d^2(s_i, T \star m_k)}{2 \cdot \sigma^2}\right)$$

The limit of this term for a low variance is obviously:

$$\lim_{\sigma^2 \rightarrow 0} r_{ijk} = \begin{cases} 0 & \text{if } d^2(s_i, T \star m_j) < d^2(s_i, T \star m_k) \\ +\infty & \text{if } d^2(s_i, T \star m_j) > d^2(s_i, T \star m_k) \end{cases}$$

Then, if $T \star m_j$ is the closest point (w.r.t. s_i), all r_{ijk} terms have a null limit, so that the limit of $\overline{(A_T)_{ij}}$ is 1. Otherwise, there exists a r_{ijk} with an infinite limit, so that the limit of $\overline{(A_T)_{ij}}$ is 0. Therefore, EM algorithm behaves as standard ICP.

7.2 EM limit for a high variance

In this section, we show that the EM algorithm simply aligns the barycentres and the inertia tensors (weighted by the a-priori probabilities of points) for a high variance. Let $\alpha = \frac{1}{2 \cdot \sigma^2}$ be the variable that tends toward 0 and $D_{ij} = d^2(s_i, T \star m_j) = \|s_i - (R \cdot m_j + t)\|^2$. The criterion 7 can be rewritten as:

$$C(T) = - \sum_i \log \left(\sum_j \overline{\pi_{ij}} \cdot p(s_i | m_j, T) \right) = - \sum_i \log \left(\sum_j \overline{\pi_{ij}} \cdot \exp(-\alpha \cdot D_{ij}) \right)$$

7.2.1 Translation part

The first order Taylor expansion of this criterion w.r.t. α is:

$$\begin{aligned} C(T) &= - \sum_i \log \left(\sum_j \overline{\pi_{ij}} \cdot \exp(-\alpha \cdot D_{ij}) \right) \\ &= - \sum_i \log \left(\sum_j \overline{\pi_{ij}} \cdot (1 - \alpha \cdot D_{ij} + O(\alpha^2)) \right) \\ &= - \sum_i \log \left(1 - \alpha \cdot \sum_j \overline{\pi_{ij}} \cdot D_{ij} + O(\alpha^2) \right) \\ &= \alpha \cdot \sum_{ij} \overline{\pi_{ij}} \cdot D_{ij} + O(\alpha^2) \end{aligned}$$

Then, for a low α (e.g. for a high variance), minimising the criterion is equivalent to minimising $\sum_{ij} \overline{\pi_{ij}} \cdot D_{ij} = \sum_{ij} \overline{\pi_{ij}} \cdot d^2(s_i, T \star m_j) = \sum_{ij} \overline{\pi_{ij}} \cdot \|s_i - (R \cdot m_j + t)\|^2$. As usual, the optimal translation aligns the weighted barycentres:

$$t = \frac{\sum_{ij} \overline{\pi_{ij}} \cdot s_i}{\sum_{ij} \overline{\pi_{ij}}} - R \frac{\sum_{ij} \overline{\pi_{ij}} \cdot m_j}{\sum_{ij} \overline{\pi_{ij}}} = \overline{s_i} - R \cdot \overline{m_j}$$

7.2.2 Rotation part

Reintroducing the translation into the criterion and using barycentric coordinates (each s_i is replaced by $s_i - \bar{s}$, each m_j is replaced by $m_j - \bar{m}$) leads to the following expression: $D_{ij} = \|s_i - R.m_j\|^2$. Thus, we are left with the minimisation of:

$$\sum_{ij} \bar{\pi}_{ij} . D_{ij} = \sum_{ij} \bar{\pi}_{ij} . \|s_i - (R.m_j)\|^2 = \sum_{ij} \bar{\pi}_{ij} . (\|s_i\|^2 + \|(R.m_j)\|^2 - 2.s_i^t . R.m_j)$$

As $\|s_i\|^2$ and $\|(R.m_j)\|^2 = \|m_j\|^2$ are constant, we can equivalently maximise $\sum_{ij} \bar{\pi}_{ij} . (s_i^t . R.m_j) = \sum_{ij} \bar{\pi}_{ij} . Tr(R.m_j . s_i^t) = Tr(R.K^t)$ with $K = \sum_{ij} \bar{\pi}_{ij} . s_i . m_j^t$.

However, when $\bar{\pi}_{ij}$ is separable (i.e. $\bar{\pi}_{ij} = \bar{\pi}_i . \bar{\pi}_j$, which is the case when using uniform priors, as in our application), K is equal to $(\sum_{ij} \bar{\pi}_{ij}) . \bar{s} . \bar{m}^t$, thus null since we are now in barycentric coordinates. Consequently, the first order expansion of our criterion is not sufficient to determine the rotation. In this case, we need to write the second order Taylor expansion:

$$\begin{aligned} C(T) &= - \sum_i \log \left(\sum_j \bar{\pi}_{ij} . (1 - \alpha . D_{ij} + \frac{1}{2} \alpha^2 D_{ij}^2 + O(\alpha^3)) \right) \\ &= - \sum_i \log \left(1 - \alpha . Cte + \frac{1}{2} \alpha^2 \sum_j \bar{\pi}_{ij} . D_{ij}^2 + O(\alpha^3) \right) \\ &= - \sum_i \left(\alpha . Cte + \frac{1}{2} \alpha^2 (\sum_j \bar{\pi}_{ij} . D_{ij}^2 - Cte^2) \right) + O(\alpha^3) \end{aligned}$$

We finally have to maximise:

$$\begin{aligned} \sum_{ij} \bar{\pi}_{ij} . D_{ij}^2 &= \sum_{ij} \bar{\pi}_{ij} . \left(\|s_i - (R.m_j)\|^2 \right)^2 \\ &= \sum_{ij} \bar{\pi}_{ij} . \left(\|s_i\|^2 + \|m_j\|^2 - 2.s_i^t . R.m_j \right)^2 \\ &= \sum_{ij} \bar{\pi}_{ij} . \left(\|s_i\|^2 + \|m_j\|^2 \right)^2 - 4 . \sum_{ij} \bar{\pi}_{ij} . \|s_i\|^2 . s_i^t . R.m_j \\ &\quad - 4 . \sum_{ij} \bar{\pi}_{ij} . \|m_j\|^2 . s_i^t . R.m_j + 4 . \sum_{ij} (s_i^t . R.m_j)^2 \end{aligned}$$

The first term is constant, the second term equals to

$$-4 . \sum_i \bar{\pi}_i . \|s_i\|^2 . s_i^t . R . \left(\sum_j \bar{\pi}_j m_j \right) = -4 . \sum_i \bar{\pi}_i . \|s_i\|^2 . s_i^t . R . \left(\sum_j \bar{\pi}_j \right) . \bar{m}$$

and is thus null since we are in barycentric coordinates, so is the third term. Finally, we are left with the maximisation of the last term:

$$\begin{aligned} \sum_{ij} \bar{\pi}_{ij} (s_i^t . R.m_j)^2 &= \sum_{ij} \bar{\pi}_{ij} (s_i^t . R.m_j . m_j^t . R^t . s_i) \\ &= \sum_i \bar{\pi}_i (s_i^t . R . (\sum_j \bar{\pi}_j . m_j . m_j^t) . R^t . s_i) \\ &= Tr(R . (\sum_j \bar{\pi}_j . m_j . m_j^t) . R^t . (\sum_i \bar{\pi}_i . s_i . s_i^t)) \\ &= Tr(R . T_m . R^t . T_s) \end{aligned}$$

where T_m and T_s are the scene and model inertia tensors. To account for the orthonormal constraints of the rotation matrix, we have to add an additional term in the Lagrangian:

$$\Lambda(R) = \frac{1}{2}Tr(R.T_m.R^t.T_s) - \frac{1}{2}Tr(L(R.R^t - Id))$$

where L is a symmetric matrix of Lagrange multipliers, to take into account constraint on R , which must be orthogonal. Expanding this Lagrangian gives:

$$\Lambda(R + \delta R) = \Lambda(R) + \frac{1}{2}Tr(\delta R.T_m.R^t.T_s + Tr(R.T_m.\delta R^t.T_s) - \frac{1}{2}Tr(L.R.\delta R^t + L.\delta R.R^t)$$

By definition of the derivative, we have $\Lambda(R + \delta R) = \Lambda(R) + Tr\left(\frac{\partial \Lambda}{\partial R}\delta R\right)$. Thus, the optimum rotations are characterised by:

$$\frac{\partial \Lambda}{\partial R} = 0 = T_s.R.T_m - L.R \quad (13)$$

Let $T_m = U.D_m.U^t$ and $T_s = V.D_s.V^t$ be diagonalisations of the data inertia tensors and $Q = V^t.R.U$, $M = V^t.L.V$ (remember that T_m , T_s , L and M are symmetric, U , V , R , Q are orthogonal, and D_m and D_s are diagonal). Equation 13 becomes: $D_s.Q.D_m = Q.M$. Assuming that the eigenvalues d_{m_i} of D_m are strictly positive, we can rewrite that as: $Q^t.D_s.Q = M.D_m^{-1}$. Thus, the matrix $M.D_m^{-1}$ is obviously symmetric: $M.D_m^{-1} = D_m^{-1}.M$. Since M and D_m commute, they can be diagonalised in the same coordinate system, here the canonical one: M is thus a diagonal matrix D verifying $Q^t.D_s.Q = D.D_m^{-1}$.

Finally, we can conclude that Q is a rotation that exchanges rows or columns (i.e. a rotation of 90 or 180 degrees) and we have $d_i = \pm d_{s_i}.d_{m_{\pi(i)}}$ where $\pi(i)$ is a permutation of the indices. Reporting the values of L and R in the criterion gives $2\Lambda_{optimal} = Tr(D) = \sum_i \pm d_{s_i}.d_{m_{\pi(i)}}$. Assuming that the eigenvalues d_{s_i} and d_{m_i} of the inertia tensors are ordered by *strictly decreasing* values, the maximal criterion is obtained for $\pi(i) = i$ and a positive sign of d_i (thus $Q = Id$ and $R = V.U^t$) with value $\sum_i d_{s_i}.d_{m_i}$. if we are looking for a proper rotation and if the determinant of $V.U^t$ is -1, the maximum criterion is obtained (in 3D) by $d_3 = -d_{s_3}.d_{m_3}$ (i.e. for $R = V.Diag(1, 1, -1).U^t$).



Unité de recherche INRIA Sophia Antipolis
2004, route des Lucioles - BP 93 - 06902 Sophia Antipolis Cedex (France)

Unité de recherche INRIA Lorraine : LORIA, Technopôle de Nancy-Brabois - Campus scientifique
615, rue du Jardin Botanique - BP 101 - 54602 Villers-lès-Nancy Cedex (France)

Unité de recherche INRIA Rennes : IRISA, Campus universitaire de Beaulieu - 35042 Rennes Cedex (France)

Unité de recherche INRIA Rhône-Alpes : 655, avenue de l'Europe - 38330 Montbonnot-St-Martin (France)

Unité de recherche INRIA Rocquencourt : Domaine de Voluceau - Rocquencourt - BP 105 - 78153 Le Chesnay Cedex (France)

Éditeur
INRIA - Domaine de Voluceau - Rocquencourt, BP 105 - 78153 Le Chesnay Cedex (France)
<http://www.inria.fr>
ISSN 0249-6399